Comparative Performances of Two Hypersonic Deceleration Devices

L. W. Sims,* C. H. Bursey Jr.,† and R. J. Berman‡
General Electric Company, Philadelphia, Pa.

Nomenclature

A = reference area, base area
C_D = drag coefficient
D = base diameter
M = Mach number
q = dynamic pressure
R = radius
V = velocity
W = vehicle weight
X = distance aft of entry vehicle base
β = ballistic coefficient, W/C_DA
β_{RATIO} = (W/C_DA) spoilers/(W/C_DA) body alone
γ = path angle

Subscripts

E,l,∞ = entry, local, and freestream, respectively
b,N = base and nose, respectively

In past studies, several types of decelerators have been considered for application to the recovery of high-performance vehicles. On the basis of such studies and on test data, body attached spoilers and a trailing wake conical device (drogue) are compared in the present Note (Fig. 1). Both of these devices are rigid and nonflexible, but depolyable. The relative effects of size, drag effectiveness, and deployment loads are considered. The basic objective is to size the systems to be compatible with a subsonic parachute for the final recovery stage.

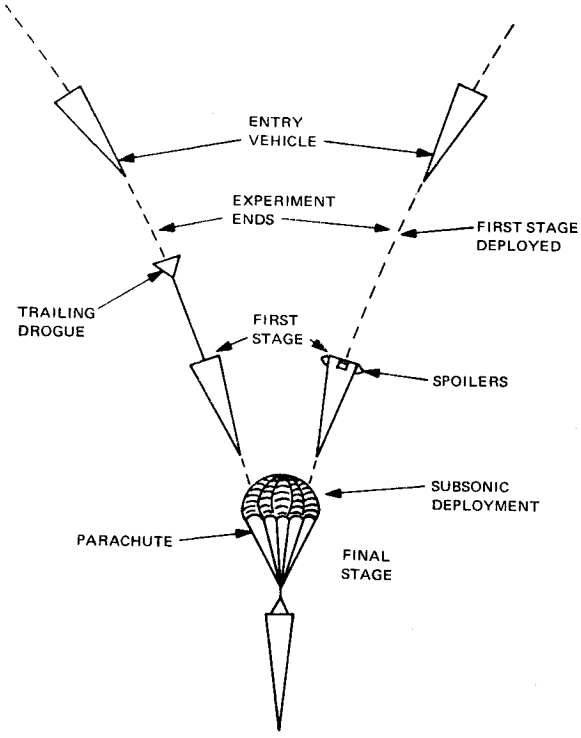

Fig. 1 Recovery sequence schematic.

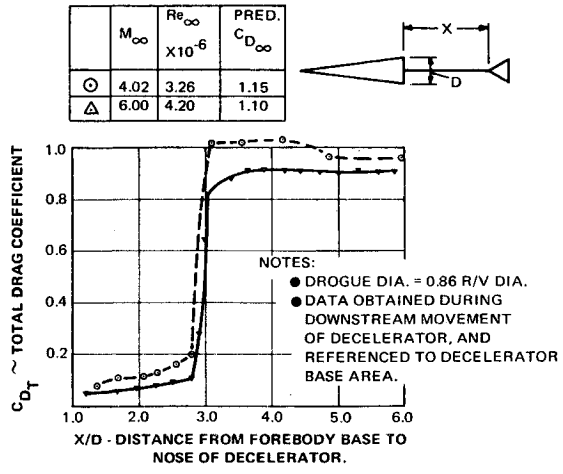

Fig. 2 Drag coefficient of a 45° half-angle conical decelerator associated with location in wake.

Decelerator Aerodynamics

Trailing rigid devices (called trailing wake drogues) such as large vertex-angle cones, conical rings, and plates have been investigated as decleration devices in wind-tunnel tests.[2–4] The strong effects of decelrator position behind the forebody and of Mach number shown in Fig. 2 have been demonstrated in numerous ground and flight tests to Mach 6 for both laminar and turbulent wakes.[3,4] Although many conical shaped devices will provide a satisfactory first stage decelerator, a 45° half-angle cone is assumed for purposes of the present study. A rigid, extensible tow rod is used to deploy and to attach the trailing device to the forebody. At close-in wake positions (Fig. 3) drag is low because of the separated low-energy flow ahead of the declerator during this time. The drag rise is nearly instantaneous when the wake closes (Fig. 2), and a normal supersonic wake flowfield engulfs the trailing decelerator. For full performance of the trailing drogue at $X/D = 4$ the upper curve shown in Fig. 3 is used; it represents a mean of typical turbulent wake drag data available from tests, supplemented by estimates based upon wake flow field measurements.[7]

The second major type of aerodynamic deceleration is the body-attached drag brake comprising aerodynamic surfaces that can be deployed into the flow. These drag brakes set up a complex flowfield with several distinct regions consisting

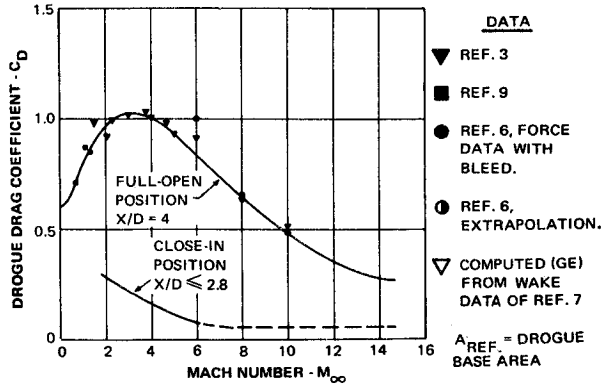

Fig. 3 Wake drogue drag coefficient variation with Mach number −45° half angle cone drogue at $X/D = 4$.

Presented as Paper 10-1207 at the AIAA Aerodynamic Deceleration Systems Conference, Dayton, Ohio, September 14–16, 1970; submitted October 5, 1970; revision received December 29, 1970.

* Consulting Engineer, Aerodynamics Laboratory. Associate Fellow AIAA.
† Consulting Engineer, Flight Dynamics and Performance Laboratory. Member AIAA.
‡ Supervising Engineer, Aerodynamics Laboratory, Re-Entry and Environmental Systems Division. Member AIAA.

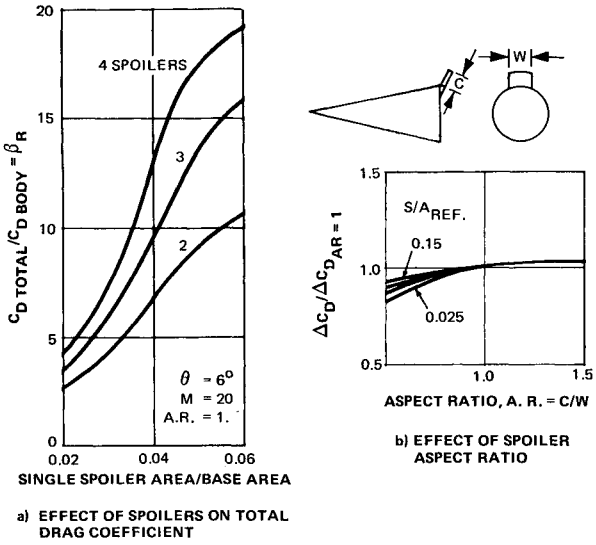

Fig. 4 Spoiler effectiveness.

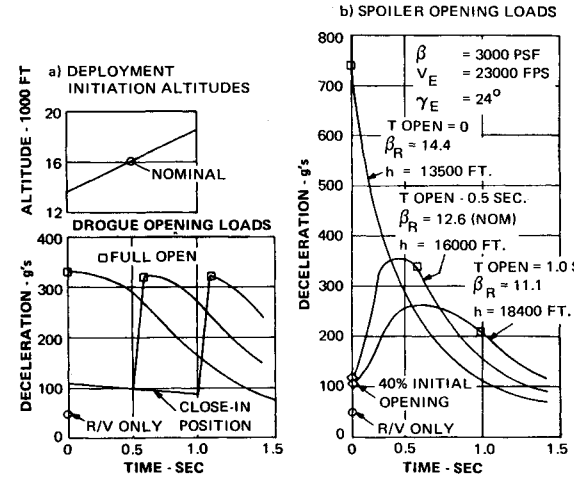

Fig. 6 Full drogue/spoiler opening loads comparison.

of the undisturbed conical body flow, the separated flow region in front of the drag brake, the front face of the brake in the separated flow region, and behind the shock caused by the drag brake itself. The techniques for estimating the flow characteristics in these regions and the performance of the drag brakes have been presented in Ref. 1. This analytical technique together with experimental ground test data,[1] have been used to determine the drag performance of this decelerator brake system. The performance is a function of the brake size; however, the aspect ratio of the brake determines what portion of the brake is submerged within the separated flow regime, and the location and number of drag brakes influence the interference effects of one drag brake on the other. Figure 4a presents drag coefficient vs area ratio for 2, 3, and 4 drag-brake systems when the aspect ratio is 1.0. The effects of aspect ratio are shown in Fig. 4b.

Since response times are critical (i.e., if no attempt were made to recover the vehicle at the maximum dynamic pressure point of the trajectory, the vehicle would impact in $\sim$2 sec), the behavior of the drag brake during the opening time interval is critical in the evaluation of the system. This behavior is a function of the boundary-layer and shock layer characteristics, particularly the dynamic pressure ratio q_l/q_∞, and the geometry of the drag brake. Also, as the drag brake deploys, bow-shock impingement or interaction with the brake may cause high loads and heating. The Mach number decreases rapidly as the brake extends, however, causing the bow shock to move away from the brake and alleviate the interaction condition. Figure 5 presents the drag history for the nominal vehicle (β = 3000) clean and with the full drogue deployed and for the corresponding spoiler configuration required for recovery from an altitude of 16,000 ft (V_e = 23,000 fps, γ_e = −24°).

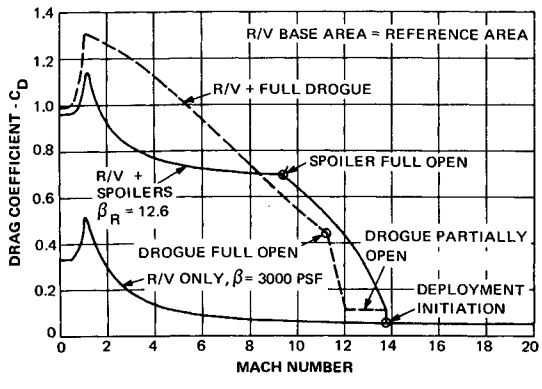

Fig. 5 Comparison of total drag coefficient with and without first stage recovery device.

Comparature Performance

In this analysis, it is assumed that the base area used for aerodynamic coefficient reference purposes and the cone angle are held constant, but a change in C_D is achieved by

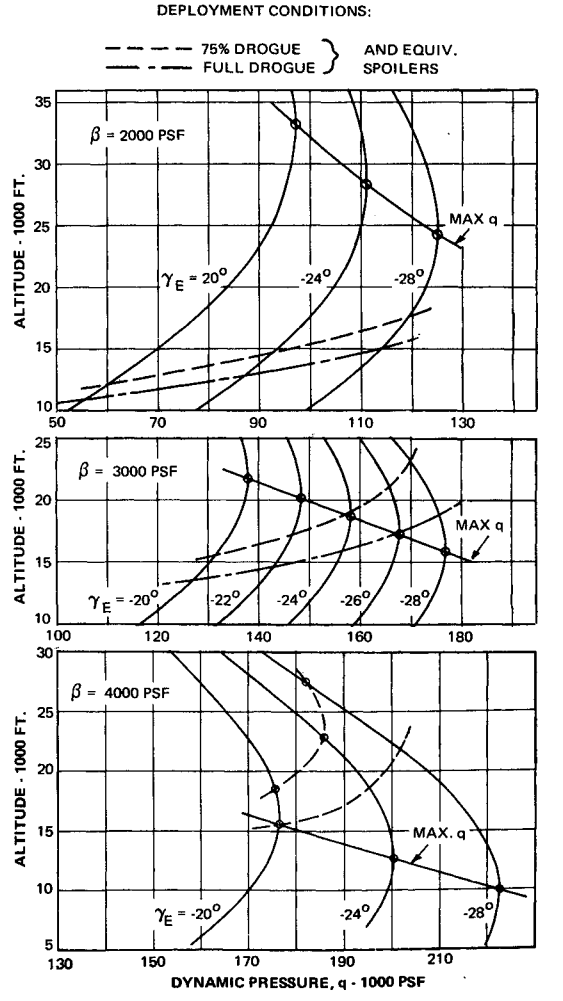

Fig. 7 Dynamic pressure variation with altitude and deployment initiation conditions, β = 2000, 3000, and 4000 psf, V_E = 23,000 fps.

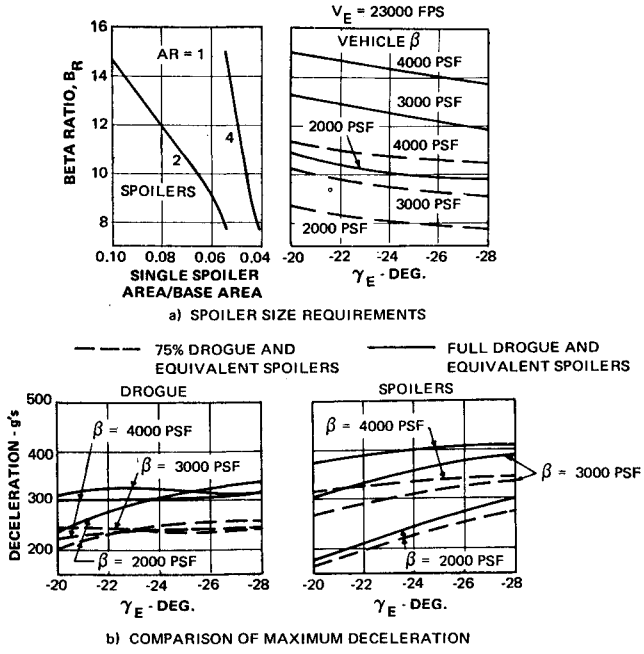

Fig. 8 Drogue and spoiler comparisons.

varying the nose radius. Table 1 defines the ballistic coefficient variables used.

A White Sands model atmosphere is used in performance computations and final recovery is accomplished by the use of a subsonic parachute deployed at Mach 0.9 at an altitude of 6000 ft.

The opening times of the drogue and spoilers were selected by comparing performance (i.e., altitude required for deployment initiation, opening air loads, and considering the type of activating mechanism required for deployment). First, the deployment altitudes required for full drogue deployment and the resulting air loads were determined for opening times of 0.0, 0.5, and 1.0 sec (Fig. 6a). These data show that the drogue maximum air loads experienced are insensitive to opening time. Therefore, an opening time of 0.5 sec was selected on the basis of performance and the finite time required for drogue extension. Using the same deployment initiation conditions and opening times used for the drogue, spoilers were sized to match the drogue performance. This results in a variation in spoiler size since the spoiler drag characteristics are different from that of the drogue. Comparative opening air loads and spoiler β ratios are shown in Fig. 6b. The combination of a high spoiler β ratio required for the low-altitude deployment and "instant opening" results in extremely high air loads for the spoilers. However, the spoiler opening airloads may be significantly reduced by a programed spoiler deployment. While the spoiler opening sequence and timing have not been optimized, it is felt that an "instant" spoiler opening of 40% (in order to minimize the ineffective low dynamic pressure region in the boundary layer) followed by a 0.5 sec opening time provides a fair basis for drogue/spoiler recovery performance comparisons.

The dynamic pressure variations with altitude for β = 2000, 3000, and 4000 psf are shown for entry path angles which vary from $-20°$ to $-28°$ in Fig. 7. The deployment initiation altitudes which yield subsonic parachute deployment conditions are shown on these curves for both a full drogue and a 75% area drogue. Computation indicates that from 82 to 99% of stagnation-point heating and from 66 to 98% of turbulent side heating are represented by the potential recovery conditions considered.

Table 1 RV characteristics

β, psf	A_{ref}, ft^2	R_N/R_b	$C_{D,a}$	Wt, lb
2000	1.767	0.200	0.0767	271
3000	1.767	0.14	0.0547	290
4000	1.767	0.05	0.0440	311

[a] Defined at Mach = 20, Altitude = 75,000 ft.

Spoilers have been sized to match the drogue performance and the results are summarized in Fig. 8a. From this figure, the spoiler size, using either 2 or 4 spoilers, may be determined for the range of vehicle β's and entry path angles considered.

A summary comparison of the maximum deceleration experienced during deployment is shown in Fig. 8b. The drogue maximum deceleration is rather insensitive to variations in entry path angle and β, but does vary with drogue effectiveness (i.e., full drogue vs 75% drogue). It should be noted that the maximum drogue deceleration occurs at the instant of full drogue deployment (Fig. 6a) and results from the assumption of a step function in the drogue drag coefficient at the time of flow attachment (see Fig. 5). The insensitivity of the drogue to β and γ_E variations results from compensating variations in opening dynamic pressure and Mach-dependent drogue drag coefficient level. The spoiler loads are not Mach number dependent since the full-open spoiler drag coefficient is assumed to be constant with Mach number. For a given opening schedule, the spoiler loads are a function of size as given in Fig. 8a and dynamic pressure as shown in Fig. 7. Figure 8b shows that the spoiler loads are, in general, higher than those of the drogue for the same recovery requirements. However, a reduction in the spoiler loads shown is possible by increasing the opening time and/or deployment altitude, as indicated by Fig. 6a. In regard to loads control, it is felt that the spoiler system offers more flexibility than the drogue.

Summary

Drogue deployment initiation conditions necessary for RV recovery have been determined for an RV β range of 2000 to 4000 psf and γ_E's from -20 to $-28°$. Spoilers have been sized to match the drogue performance and the spoiler area is provided (referenced to RV base area) for either 2 or 4 symmetrically mounted spoilers.

Trailing drogue maximum air loads are found to be insensitive to the deployment ("opening") time, vehicle ballistic coefficient and entry path angle. Spoiler loads are highly sensitive to opening time, but may be controlled by means of a programed opening procedure. Trailing drogue loads are sensitive to the drogue effectiveness (prediction). For the nominal vehicle β of 3000 psf, and γ_E of 24°, 4 spoilers each having 5% of the base area are equivalent to a full drogue in recovery capability. Both first stage devices will provide comparable end conditions, which will enable the use of a subsonic parachute final stage.

References

[1] Steck, J. H., Berman, R. J., and Blanco, T. T., "Recovery of High Performance Re-entry Vehicles by Drag Brakes Plus Parachutes," *Journal of Spacecraft and Rockets*, Vol. 4, No. 6, June 1967, pp. 746–750.

[2] "Recovery Environment Study Program," SAMSO-TR-68-12, Final Report, Vol. II, Jan. 1968, NAFB, Calif.

[3] Coats, J. D., "Static and Dynamic Testing of Conical Trailing Decelerators for the Pershing Re-entry Vehicle," TN-60-188, Oct. 1960, Arnold Engineering Development Center, Tullahoma, Tenn.

[4] Charczenko, N. and McShera, J. T., "Aerodynamic Characteristics of Towed Cones Used as Decelerators at Mach Numbers From 1.57 to 4.65," TN D-994, Dec. 1961, NASA.

[5] Minerva, P. A. and Turner, R. D., "Recovery System Requirements for High Performance Re-entry Vehicles," *Proceedings for the AIAA Aerodynamic Deceleration Systems Conference*, AIAA, New York, 1966, p. 188.

[6] "Decelerator Performance Study Program," Final Report, SAMSO-TR-70-48, March 1970, TRW Systems Group, NAFB, Calif.

[7] Martellucci, A. et al., "Experimental Study of Near Wakes," BSD-TR-67-229, Vol. I, Nov. 1967, NAFB, Calif.
[8] Yeager, D. R., "Results of a Mach 8 Wind Tunnel Test to Determine Drag and Static Stability for a Nine-Degree Cone with Spoilers," GE RS ATDM 66-5, April 1966, General Electric Co., Philadelphia, Pa.
[9] Heinrich, H. G. and Hess, R. S., "Drag Characteristics of Plates, Cones, Spheres and Hemispheres in the Wake of a Forebody at Transonic and Supersonic Speeds," RTD-TDR-63-4242, Dec. 1964, Wright-Patterson Air Force Base, Ohio.

Space Interceptors: An Investigation of Seven Main Parameters

ROBERT SALKELD*
Los Angeles, Calif.

Nomenclature

D = incident dose of nuclear radiation, rad
F = interceptor thrust, lb
g = acceleration of gravity, naut miles/sec^2
I = interceptor specific impulse, sec
k = warhead radiation flux coefficient, rad-naut miles^2/megaton
m = warhead yield coefficient, megatons/lb
R = radius of intercept ($r + x$), naut miles
r = warhead kill radius, naut miles
t = time to intercept, sec
V = intercept volume, naut miles^3
W = $W(t) = w_i + w_w + w_p(t)$, interceptor gross weight, lb
w = weight, lb
X_{Tt} = distance of target from origin of interceptor's flight at intercept time
x = straight line distance travelled by interceptor, naut miles
y = mw = warhead yield, megatons
ρ = area density of target shielding (lb/ft^2)
λ = interceptor inert factor, $w_i/(w_i + w_p)$

Subscripts

b = condition at burnout time
i = interceptor inert components
N = neutron radiation
p, w = interceptor propellant and warhead, respectively
$t, 0$ = conditions at times t and $t = 0$, respectively
γ = gamma radiation

Introduction

THE effectiveness of an interceptor can be measured by the volume within which it can perform intercept in a given time. This "reach" is in general made up of two components: 1) the destructive mechanism of the warhead, which establishes a kill-radius r about the interceptor, and 2) the propulsive maneuvering capability by which the interceptor moves to the target vicinity. In a gravity field, both the paths of the interceptor and the intercept volumes generated by them can become geometrically complex, especially for long intercept times.[1] Even so, useful parametric trends can be obtained from an analysis which assumes gravity-free space. In this case, the interceptor "reach" is merely $R = r + x$, and the intercept volume is the sphere generated by R. Intercept is assumed to occur if $X_{Tt} \leq R$. This simplified analysis allows direct investigation of the relationships among seven key parameters: 1) intercept volume V; 2) intercept time t; 3) r; 4) interceptor gross weight W_0; 5) propellant weight w_p; 6) specific impulse I; and 7) thrust level F.

Received October 13, 1970; revision received November 16, 1970.

* Consultant, 410½ Landfair Avenue, Westwood Village. Associate Fellow AIAA.

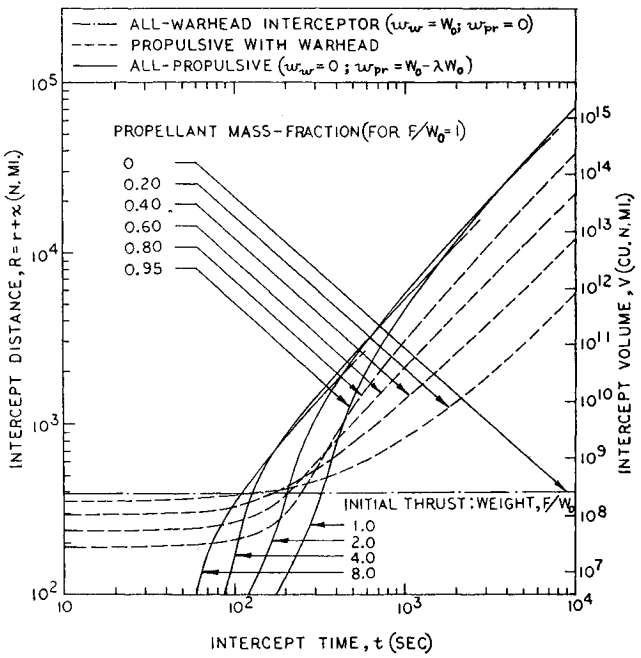

Fig. 1 Oxygen-hydrogen interceptors: intercept distance and volume vs intercept time for various warhead-propulsion combinations, and thrust: weight ratios (see Table 1 for assumptions).

Analysis

For straight-line flight through gravity-free space,

$$\dot{x}_{(t \leq t_b)} = gI \ln W_0/W_t,\ W_t = W_0 - (F/I)t \tag{1}$$

and integration gives

$$x_{(t \leq t_b)} = gI[(t - W_0 I/F) \ln W_0/W_t + t] \tag{2}$$

At burnout, $t_b = w_p I/F$, and $W_t = W_0 - w_p$.

After burnout, the interceptor continues on at the burnout velocity, $\dot{x}_{tb}$, so that

$$x_{(t \geq t_b)} = x_{tb} + \dot{x}_{tb}(t - t_b) \tag{3}$$

$$= gI\{(t - W_0 I/F) \ln[W_0/(W_0 - w_p)] + w_p I/F\} \tag{3a}$$

Warhead kill radius

If a non-nuclear warhead is used, r is quite limited, probably to the order of a mile. If a nuclear radiation mechanism is used, r may be hundreds of miles. Certain data pertaining to lethal dosages of gamma and neutron radiation[2] will be used here to construct an illustrative expression for r against manned vehicles. Thus, from Ref. 2 (Sec. 8.101) the general expression for nuclear bursts in the atmosphere is

$$D \approx k(y/r^2)e^{-r/\text{const}} \tag{4}$$

where the exponential factor accounts for atmospheric attenuation. In space, there is no attenuation, and substituting $y = mw_w$,

$$D \approx kmw_w/r^2 \tag{5}$$

and

$$r \approx \{(km/D)[W_0 - w_p/(1 - \lambda)]\}^{1/2} \tag{6}$$

To estimate k and m, we use Eq. (5) and the data given in